Received: 29 October 2016 | Revised: 29 March 2017 | Accepted: 5 April 2017

DOI: 10.1002/qua.25390

FULL PAPER

WILEY International Journal of QUANTUM CHEMISTRY

A quartic force field coordinate substitution scheme using hyperbolic sine coordinates

Diego J. Alonso de Armiño[1] | Carlos M. Bustamante[2]

[1]INQUINOA (CONICET-UNT) San Lorenzo 456, Tucumán, T4000CAN, Republica Argentina

[2]Instituto de Quimica-Fisica, Facultad de Bioquimica, Quimica y Farmacia, Universidad Nacional de Tucuman, San Lorenzo 456, T4000CAN, San Miguel de Tucumán, Tucumán, Argentina

Correspondence
Diego J. Alonso de Armiño, INQUINOA (CONICET-UNT) San Lorenzo 456, Tucumán, T4000CAN, Republica Argentina.
Email: diegoarmino@gmail.com

Abstract

Quartic force fields (QFF) are currently the most cost-effective method for the approximation of potential energy surfaces for the calculation of anharmonic vibrational energies. It is known, although, that its performance can be less than satisfactory due to limitations related to slow convergence of the series. In this article, we present a coordinate substitution scheme using a combination of Morse and sinh coordinates, well adapted for its use with cartesian normal coordinates. We derive expressions for analytical integrals for use in VSCF and VCI calculations and show that the simultaneous substitution of symmetric and antisymmetric normal coordinates by Morse and sinh coordinates, respectively, significantly improves the vibrational transition frequencies for these modes in a well-balanced fashion. The accuracy of this substitution scheme is demonstrated by comparing one and two-dimensional sections of substituted and unsubstituted QFF with *ab initio* potential energy grids, as well as with vibrational energy calculations using as test cases two well-studied benchmark molecules: water and formaldehyde. We conclude that the coordinate substitution scheme presented constitutes a very attractive alternative to simple QFFs in the context of cartesian normal coordinates.

KEYWORDS

quantum chemistry, quartic force fields, vibrational structure

1 | INTRODUCTION

The calculation of accurate potential energy surfaces (PES) is certainly a crucial part of the computation of anharmonic vibrational energies and wavefunctions of molecular systems. Grid representations[1] of the PES are usually the most accurate option, although its high computational cost limits its application to very small systems, as the number of energy evaluations necessary for a complete grid rises exponentially with the number of normal modes. This limitation can be reduced somewhat by the use of *N*-mode coupling representations,[2–4] or more recently, adaptive sparse grid expansions.[5] Grids may be used directly, or converted into an analytical expression either by fitting[6] or interpolation[7] procedures. For example, very high accuracy have been obtained using reproducing kernel Hilbert space interpolation coupled to a grid representation for triatomic reactive systems.[8] Grid methods, even the most efficient examples of them, are still limited to small systems, so alternatives are needed for bigger molecules.

Quartic force fields (QFF), this is, fourth order Taylor expansions of the potential with respect to the normal coordinates of the system, currently represent the best trade-off of accuracy and computational cost for the representation of molecular potential energy surfaces (PES) for anharmonic vibrational structure applications. The efficiency of the QFF scheme comes from the possibility of calculating the expansion coefficients by numerical differentiation of the potential, analytical gradients, or Hessians, if available. Moreover, recently Ramakrishnan and Rauhut presented an efficient scheme for computing QFFs from multimode expansions.[9] In this way, a complete QFF can be obtained at a small fraction of the cost that a potential grid would require. QFFs usually show a slow convergence of the Taylor series, which translates in noticeable loss of accuracy, which in many cases may be insufficient even for the calculation of fundamental vibrational transitions, introducing errors in the order of tens of wavenumbers in the vibrational energies compared to grid methods.[1,10–13] Proton stretching modes in particular are very challenging for QFFs. In the case of symmetric modes, for example, the potential energy tends to an asymptotic limit as the stretch coordinate is displaced toward positive or negative infinity, depending on the phase of the normal mode, whereas the Taylor series in normal coordinates will always tend to positive or negative

infinite energies in the limit of infinite displacements of the coordinate. A fourth order expansion often falls short of an accurate representation of the potential along these modes. Using higher order polynomials is usually out of the question, because of their cost, and numerical accuracy considerations. Modified Shepard Interpolation (MSI) schemes were proposed to improve the performance of QFFs,[14–16] and have since been successfully applied to many molecular systems.[1,17–20] Although significant improvements were obtained for vibrational frequencies relative to simple QFF schemes, this method requires some prior knowledge of the PES to place additional reference points,[21]and although some methods for automatic selection of those points have been proposed,[22] the scheme still implies a significant increment in computational cost. A very interesting way of improving QFFs was implemented by Dateo et al.[23] and later by Fortenberry et al.[13,24–26] based on the early work by Watson,[27] Meyer et al.,[28] and Carter and Handy,[29] in the context of internal valence coordinates. The scheme consists of substituting single bond stretching coordinates with Morse coordinates, which present the correct asymptotic behavior, obtaining excellent fits for the vibrational frequencies to within a few cm^{-1} of experiment. What makes this approach so attractive is the fact that unlike, for example, MSI, there is no increase in the computational cost relative to that of a simple QFF and is also much simpler to implement and to use. Building on these ideas, Burcl et al.,[10] presented a similar scheme especially adapted for its use in the context of cartesian normal coordinates. In this case, Morse coordinate substitution can only be performed on symmetric normal coordinates, which may lead to an imbalance in the representation of stretching modes, as Morse coordinates do not present the correct limiting behavior for substitution into antisymmetric stretch normal coordinates. For this reason, Burcl et al. proposed the use of Gaussian coordinates for these, following a previous paper by Carter and Handy[30] proposing the use of hyperbolic tangent coordinates for the same purpose. Gaussian and tanh coordinates, however, should be better adapted for cases when the potential along the normal coordinate to be substituted shows even parity and a dissociative asymptotic limit. In cases where this is not so, the coordinate substitution may still provide a poor convergence radii for the potential. Moreover, the integrals involving Gaussian or tanh coordinates for the solution of the variational vibrational structure equations must be solved numerically, which complicates its implementation in codes that make use of analytic integrals, such as our own.

Following the work by Burcl et al.,[10] we present here a new coordinate substitution scheme, based in a combination of hyperbolic sine and Morse coordinates, especially adapted for its implementation with cartesian normal coordinates using analytical integrals for the solution of the variational structure equations.

In section 2, we present a brief introduction on the theory of anharmonic vibrational energy calculations, after which, we present the theoretical framework for this article. Section 3 is concerned with computational and implementation details. Section 4 is concerned with testing the accuracy of the proposed schemes Concluding remarks are presented in section 5.

2 | THEORY

We start with a brief introduction to the vibrational self-consistent field and vibrational configuration interaction methods. Further details may be found in Refs. [31–34].

Briefly, starting from the vibrational Schrödinger equation and representing the vibrational wavefunction as a Hartree product, (i.e., a product of one-dimensional, single-mode wavefunctions or "modals," analogous to orbitals in electronic structure theory), and applying the variational principle it is possible to obtain the VSCF equations for each modal. Because the solutions (the modals) are necessary to compute the mean field potential included in the effective Hamiltonian, the VSCF equations must be solved iteratively until self-consistency.

The VSCF method only considers vibrational correlation in an averaged fashion. To account for it more explicitly, we implemented a vibrational configuration interaction (VCI) algorithm.[35] Correlated vibrational wavefunctions and energies are obtained by diagonalizing the full Hamiltonian using the virtual VSCF states as a basis set.[32,36,37]

In our implementation, a series of reference states are selected and then VSCF and VCI calculations are performed sequentially for each one, an algorithm that has been called "state-specific" VSCF/VCI, in contrast to "ground state based" (gs) VSCF/VCI in which a single calculation is performed, usually with the ground state as a reference. The state-specific (ss) version has the advantage of producing better energies compared to the gs type.

The potential is represented as a QFF in rectilinear mass-weighted normal coordinates, which can be expressed as

$$V(Q)=V_o+\frac{1}{2}\sum_{i=1}^{f} f_{ii}\ Q_i^2+\frac{1}{6}\sum_{i,j,k}^{f} f_{ijk}Q_iQ_jQ_k+\frac{1}{24}\sum_{i,j,k,l}^{f} f_{ijkl}Q_iQ_jQ_kQ_l \tag{1}$$

where f_{ii}, f_{ijk}, and f_{ijkl} are the two, three, and four modes-coupling force constants, which can be obtained by numerical differentiation of the energies, analytic gradients, analytic Hessians or by fitting procedures.

Consider now a molecule in which two bond stretching coordinates are related through symmetry. The resulting normal coordinates will be linear combinations of these two, producing a symmetric and an antisymmetric mode. The potential along each bond stretching coordinate r_1 and r_2 will be Morse-like, so it is reasonable to represent each using Morse coordinates.

$$\begin{aligned} R_1&=1-\exp\left(-\alpha_1\ r_1\right)\\ R_2&=1-\exp\left(-\alpha_2\ r_2\right)\end{aligned} \tag{2}$$

Considering that due to symmetry $\alpha_1=\alpha_2=\alpha$ and also that $r_1=r_2$ for the symmetric linear combination and $r_1=-r_2$ for the antisymmetric linear combination, it is straightforward to show that the symmetric and antisymmetric normal coordinates can be expressed as

$$Q_s=1-\exp(-\alpha\ r)$$
$$Q_a=\sinh(\alpha\ r) \tag{3}$$

So the use of hyperbolic sine coordinates for antisymmetric modes is immediately suggested by the use of Morse coordinates for single bond stretchings.

For the α factor we adopt the convention of Dateo et al. in the case of Morse coordinates.[23]

Although the symmetry considerations advanced previously are valid in many cases, an independent definition of the α factor for hyperbolic sine coordinates is more flexible. Following similar considerations as those advanced Ref. [23] and renaming as β the factor for sinh coordinates, it is simple to derive the following expression

$$\beta_i=\sqrt{\frac{f_{iiii}}{4f_{ii}}} \tag{4}$$

The only remaining task is to convert the force constants of Equation 1, which can be easily done by applying the chain rule.

At this point it is worth noticing that the procedure just outlined is not limited to molecules with only two symmetry related bond-stretch coordinates, and can in fact be applied to systems with any number of such of symmetry-related stretch coordinates without modification, as long as they form a basis for one-dimensional irreducible representations of the point group only. Moreover, it is easily shown that the procedure can also be straightforwardly generalized to produce a complete representation of bond stretchings including multidimensional irreducible representations too. This however is outside the scope of the present study and will be further explored in future works.

Our code, QUMVIA,[38,39] uses analytic expressions for the VSCF integrals in a distributed Gaussian (DG) basis set.[40]

More details may be found in Refs 40,41 for the normal coordinate case. Consider first a QFF in a combination of normal, Morse and sinh coordinates, which we call collectively R_i. The force constants F_{ii}, F_{ijk}, and F_{ijkl} are obtained from those in Equation 7 by use of the chain rule,

$$V(Q)=\frac{1}{2}\sum_{i=1}^{f}F_{ii}\ R_i^2+\frac{1}{6}\sum_{i,j,k}^{f}F_{ijk}R_iR_jR_k+\frac{1}{24}\sum_{i,j,k,l}^{f}F_{ijkl}R_iR_jR_kR_l \tag{5}$$

Where R_n is a function of Q_n, and may be equal to $(1-\exp(-\alpha_nQ_n))$, $\sinh(\beta_nQ_n)$, or simply Q_n. We need analytical expressions for integrals of the form $\langle\phi_k^{(p)}|R_k^n|\phi_k^{(s)}\rangle$, where p and s are quantum numbers, $n=1,2,3,4$ and the modals ϕ_k are linear combinations of distributed Gaussian functions.

$$\gamma_{k\mu}(Q_k)=\left(\frac{2A_{k\mu}}{\pi}\right)^{\frac{1}{4}}\exp\left[-A_{k\mu}(Q_k-Q_{k\mu})^2\right] \tag{6}$$

Where $Q_{k\mu}$ are scaled Gauss–Hermite quadrature points along the normal mode Q_k. Definitions of $A_{k\mu}$ can be found in Ref. [40]. Expanding the previous integral in terms of the DG basis functions we obtain the following expression.

$$\langle\phi_k^{(p)}|R_k^n|\phi_k^{(s)}\rangle=\sum_{\mu\nu}C_{k\mu}^pC_{k\nu}^s\langle\gamma_{k\mu}|R_k^n|\gamma_{k\nu}\rangle \tag{7}$$

Where $C_{k\mu}^p$ and $C_{k\nu}^s$ are coefficients of the expansions of $\phi_k^{(p)}$ and $\phi_k^{(s)}$, respectively. In the case of Morse coordinates, the matrix elements of R_k^n in the DG basis are.

$$\langle\gamma_{k\mu}|R_k^n|\gamma_{k\nu}\rangle=S_{\mu\nu}\sum_{m=0}^{n}\binom{n}{m}(-1)^m\ M_{\mu\nu m} \tag{8}$$

$$M_{\mu\nu m}=\exp\left(\frac{m^2\alpha^2}{4B_{\mu\nu}^2}-m\ \alpha\ D_{\mu\nu}\right) \tag{9}$$

$$D_{\mu\nu}=\frac{A_{k\mu}Q_{k\mu}-A_{k\nu}Q_{k\nu}}{B_{\mu\nu}^2} \tag{10}$$

Expressions for $B_{\mu\nu}$ and the overlap matrix elements $S_{\mu\nu}$ can be found in Ref. [40]. In a similar fashion, if R_k is defined as a sinh coordinate, the corresponding analytical expressions for the integrals are

$$\langle\gamma_{k\mu}|R_k^n|\gamma_{k\nu}\rangle=\frac{S_{\mu\nu}}{2^{n-1}}\sum_{m=0}^{(n-1)/2}(-1)^{\frac{n-1}{2}-m}\binom{n}{m}F_{\mu\nu m} \tag{11}$$

if n is odd, and

$$\langle \gamma_{k\mu}|R_k^n|\gamma_{k\nu}\rangle = \frac{1}{2^n}\binom{n}{n/2} + \frac{S_{\mu\nu}}{2^{n-1}}\sum_{m=0}^{n/2-1}(-1)^{\frac{n}{2}-m}\binom{n}{m}G_{\mu\nu m} \tag{12}$$

if n is even. Where

$$F_{\mu\nu m} = e^{\frac{(n-2m)^2\beta^2}{4B_{\mu\nu}^2}}\sinh\left((n-2m)D_{\mu\nu}\beta\right) \tag{13}$$

$$G_{\mu\nu m} = e^{\frac{(n-2m)^2\beta^2}{4B_{\mu\nu}^2}}\cosh\left((n-2m)D_{\mu\nu}\beta\right) \tag{14}$$

Analytical expressions for the matrix elements of $\langle \gamma_{k\mu}|Q_k^n|\gamma_{k\nu}\rangle$ can be found in Ref. [41].

3 | COMPUTATIONAL AND IMPLEMENTATION DETAILS

All vibrational structure calculations were performed using QUMVIA (Quantum Mechanical Vibrational Analysis) a recently written vibrational structure program developed in our group, that implements vibrational self-consistent field (VSCF) and vibrational configuration interaction (VCI) vibrational structure schemes for the calculation of anharmonic vibrational energies and wavefunctions. QUMVIA is written in Fortran 90, and is the first software package of this kind with GNU GPLv3 license and, therefore, freely available to the community through GitHub website.[42]

Quartic force fields with 3-mode couplings were calculated using Gaussian 03.[43] The structures were optimized with a "very strict" convergence criterion, followed by frequency calculation to obtain normal modes, harmonic frequencies and hessian matrix. With these data, a series of conformations distorted along each normal mode were generated using QUMVIA, and Hessian matrices were calculated for each of these using Gaussian. Finally, these Hessian matrices were used to compute 3-mode coupling QFF in QUMVIA. All 3-mode coupled QFF were computed using analytical Hessians. Quartic force fields calculations were made at the MP2/cc-pVTZ electronic structure level of theory.

Sixteen distributed Gaussian basis functions positioned at sixteen scaled Gauss–Hermite quadrature points were used for each normal mode. A VSCF energy convergence criterion of 10^{-9} Hartrees was used.

Following VSCF, a VCI computation was performed for each normal mode. Single, double, triple and quadruple modal excited VSCF virtual states were included in the VCI basis set, except in the case of water, for which only up to triple excitations were included. The maximum number of energy quanta in each excited modal was set to 6 for singles, 6 for doubles, 4 for triples, and 3 for quadruples.

4 | RESULTS AND DISCUSSION

4.1 | Accuracy of model potentials

We begin our study with a comparison between the model potentials, QFF, Morse-substituted QFF (MQFF), where Morse coordinates are used for the symmetric proton stretching normal mode and the antisymmetric normal mode is left in normal coordinates, sinh-substituted QFF (SQFF), where sinh coordinates are used for the antisymmetric proton stretching normal mode and normal coordinates are used for the rest of the potential, a Morse/sinh substituted QFF (hereon referred to as MSQFF),where both substitutions are applied simultaneously, and the actual *ab initio* potential energy surface obtained by potential energy scans along the symmetric and antisymmetric normal modes of water and formaldehyde molecules. The objective of such analysis is to assess the accuracy of substituted model potentials relative to unsubstituted QFFs and *ab initio* potential energy surfaces.

In Figure 1, we show potential energy scans, QFF and MSQFF along symmetric and antisymmetric normal modes at the MP2/cc-pVTZ electronic structure level of theory. In the case of symmetric modes (panels a and c) QFFs begin to diverge from the *ab initio* potential at low energies, while the MQFF along this mode shows a significantly improved fit to the potential energy scan. Similarly to the symmetric modes, the potential along the antisymmetric modes (panels b and d) follows a similar trend, with the SQFF (full magenta lines) showing an improved fit to the actual potential compared to QFF.

The error reduction of the MQFF relative unsubstituted QFF along the symmetric mode is 87% for formaldehyde and 82% for water. While in the case of sinh-substituted QFF along the antisymmetric mode is 94% for both formaldehyde and water. Hyperbolic sine coordinates provide, thus, an even better approximation of the potential along antisymmetric modes, than Morse coordinates do for symmetric modes for the particular cases presented here.

This kind of analysis, although undoubtedly relevant, does not guarantee that the improvement observed in these potential sections will translate into a similar one in the calculated frequencies using VSCF/VCI vibrational structure methods. Indeed, the data discussed so far only suggests similar improvements in diagonal potential matrix elements. Coupling potential matrix elements do have a strong influence in the calculated vibrational frequencies, however. We consider then, that in order to produce a more meaningful estimation of the accuracy of QFFs, it is necessary to include at least two-dimensional sections of the potential, whenever strong coupling terms arise, such as is the case for symmetric and antisymmetric modes of the test molecules at hand. Moreover, there are no published studies on the effectiveness of coordinate substitutions to model coupling regions of the potential, especially for the sinh coordinate substitution that we present in this work. It would be interesting to evaluate the accuracy of the MSQFF compared to that of QFF and *ab initio* grids in these important PES sections.

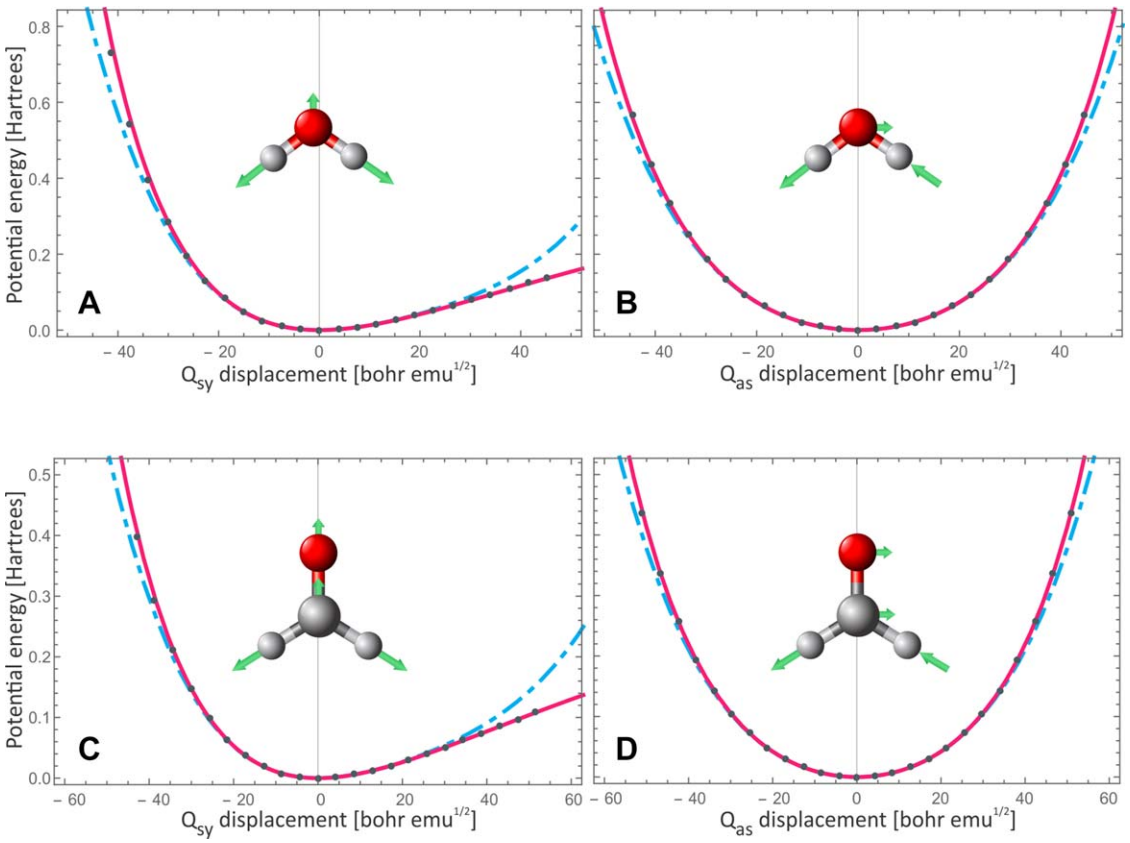

FIGURE 1 Comparison of *ab initio* potential energy scans (dark gray full circles) with standard QFF (light blue discontinuous lines) and MSQFF (magenta full lines) along symmetric (left-hand panels) and antisymmetric (right-hand panels) normal modes of water (panels A and B) and formaldehyde (panels C and D) at the MP2/cc-pVTZ electronic structure level of theory

In Figure 2, we compare QFF and MSQFF model potentials with *ab initio* bidimensional grids over C—H symmetric and antisymmetric stretching modes for formaldehyde (panels A–C) and water (panels D–F).

Comparing the *ab initio* grid (top panels a and d) with QFF (middle b and e) and MSQFF (bottom panels c and f) we can see that MSQFF produces a surface in better accordance with the actual *ab initio* potential than QFF for our test cases. Differences only begin to be noticeable for displacements in both coordinates of more than 20 bohr emu$^{1/2}$, where the sinh coordinate rises more steeply at the borders of the plot than the *ab initio* grid. This shows as a greater curvature of contour lines at upper and lower right borders of the plot, an effect of the truncation of the MSQFF at fourth order. QFF potential surface, on the other hand differs considerably at regions well within the 20 bohr emu$^{1/2}$ mark.

Figure 3 shows the absolute values of percentage errors for the surfaces of Figure 2 relative to the *ab initio* grid. We can see that QFF concentrates its accuracy along straight orthogonal directions (Qs,0) and (0,Qa) in both molecules. MSQFF on the other hand shows not only a much expanded range of validity, but, very interestingly, low error sections well inside the coupling regions in the potential energy surfaces of both molecules, most clearly seen in the case of formaldehyde (Figure 2B) along directions (Qs,Qa)=(+,+) and (+,−).

A similar feature can be observed in the case of water, where the low error region is curved along the symmetric mode (Qs) direction toward positive antisymmetric mode (Qa) values. MSQFF produces a much better representation of the coupling regions between symmetric and antisymmetric C—H stretching normal modes, when compared with a simple QFF representation for the test cases presented here. Potential surfaces of SQFF and MQFF, as well as error surfaces for water and formaldehyde are shown in Supporting Information, Figures S1 and S2, respectively. Comparing error surfaces in Figure 1 with Supporting Information S1 and S2 we can see that the former is not a simple superposition of the later. A synergic effect appears to exist in the simultaneous use of sinh and Morse.

4.2 | Vibrational frequencies

We now turn our attention to the accuracy of vibrational frequencies. With the intention of comparing the performances of QFF, MQFF, SQFF, and MSQFF for vibrational structure computations, we performed VSCF/VCI calculations using all four of the model potentials at the MP2/cc-pVTZ level of electronic structure theory for water and formaldehyde as described in the computational details section.

Table 1 shows VCI frequencies (in wavenumbers) for the fundamentals, first overtones and combination bands of water.

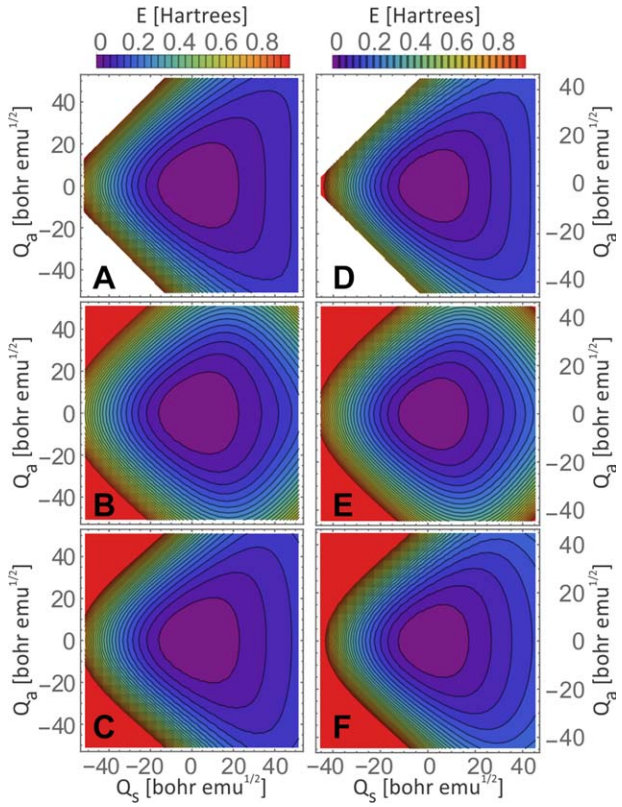

FIGURE 2 Bi-dimensional potential energy surfaces for formaldehyde (A–C) and water (D–F) showing the coupling region between the symmetric (horizontal axis, Qs) and antisymmetric (vertical axis, Qa) C—H stretching normal modes. Upper panels are *ab initio* grids (A and D), middle panels are QFF (B and E) and bottom panels are MSQFF PES (C and F) representations. The energy scale is shown at the top and has dimensions of Hartrees, while the normal mode displacements, bohr $emu^{1/2}$. White sections in panels a and d are points where the potential energy could not be evaluated due to convergence problems in the electronic structure software

Fundamental bands show significant improvements in all three coordinate-substituted potentials relative to QFF for the test cases presented. MSQFF produces the best results, with a mean absolute deviation (MAD) of only 11 cm^{-1} compared to 47 cm^{-1} for QFF, a 76% reduction. The Morse-substituted QFF, on the other hand, produces fundamental transition frequencies with a MAD reduction of only 51%, while SQFF shows a 25% improvement.

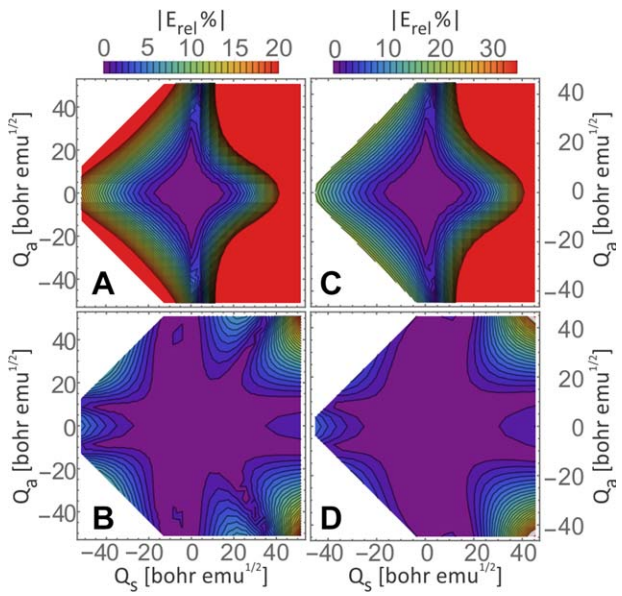

FIGURE 3 QFF (top panels a and c) and MSQFF (bottom panels b and d) relative error (%) surfaces (only absolute values are shown for the errors, for the sake of simplicity) relative to *ab initio* grid for formaldehyde (left) and water (right) for the respective V(Qs,Qa) surfaces of Figure 2

TABLE 1 VCI frequencies (cm^{-1}) of fundamental, overtone, and combination bands for water using QFF, MQFF, SQFF, and MSQFF model PES at the MP2/cc-pVTZ electronic structure level of theory

States		Model potential				Experimental[a]
		QFF	MQFF	SQFF	MSQFF	
ν_1		3719 (62)	3683 (26)	3711 (54)	3674 (17)	3657
ν_2		1579 (16)	1582 (13)	1577 (18)	1580 (15)	1595
ν_3		3820 (64)	3787 (31)	3788 (32)	3758 (2)	3756
1_2		7409 (208)	7268 (67)	7384 (183)	7220 (19)	7201
2_2		3126 (26)	3124 (28)	3120 (32)	3121 (31)	3152
3_2		7611 (166)	7524 (79)	7494 (49)	7435 (10)	7445
1_12_1		5251 (16)	5231 (4)	5236 (1)	5217 (18)	5235
2_13_1		5325 (6)	5297 (34)	5280 (51)	5257 (74)	5331
1_13_1		7499 (249)	7337 (87)	7432 (182)	7261 (11)	7250
MAD	Fundamentals	47	23	35	11	
	Overtones	133	58	88	20	
	Comb. Bands	90	41	78	34	
	Overall	90	41	67	22	

Experimental values are also given for reference. Absolute deviations from experimental values are shown in parentheses. Mean absolute deviations (MAD) for various groups of transitions are presented at the bottom of the table.
[a]References [44–56].

Interestingly, symmetric and antisymmetric transitions show simultaneous improvements in both singly-substituted quartic force fields, suggesting that each coordinate substitution by itself produces an improved representation of the coupling zones of the potential than the simple QFF model for the presented test cases.

This can be corroborated by comparing the bidimensional potential surfaces for both singly-substituted potentials, with the unsubstituted QFF (Figure S1, in Supporting Information[47]). As expected, the bending mode shows little change in all four potentials. In the case of overtone bands, MSQFF produces an 85% reduction in mean absolute deviation, with a MAD of 133 cm^{-1} for QFF compared with only 20 cm^{-1} for MSQFF. Singly-substituted potentials again show enhanced frequencies for both symmetric and antisymmetric modes, with a clear preference for the mode being substituted. MAD reductions are 56% and 34% for MQFF and SQFF, respectively.

The overall MAD reductions in the case of combination bands are 62%, 54%, and 13% for MSQFF, MQFF, and SQFF respectively. As expected, the best results are obtained for the 1_13_1 band, where the deviations are 11 cm^{-1} for MSQFF, 87 cm^{-1} for MQFF, and 182 cm^{-1} in the case of SQFF, compared with the hefty 249 cm^{-1} of QFF. The reduction of 96% in the deviation of the 1_13_1 band in the case of MSQFF (65% for MQFF and 27% for SQFF), is balanced with a strong decrement in the accuracy of the 2_13_1 combination band, which shows a very low deviation (6 cm^{-1}) when the QFF potential representation is used, and steadily worsens in going through MQFF, SQFF, and MSQFF, with deviations of 34, 51, and 74 cm^{-1}, respectively.

Table 2 shows vibrational frequencies in wavenumbers for the fundamental bands, overtones and combination bands of formaldehyde using unsubstituted QFF as well as three kinds of substituted QFFs.

Fundamental band frequencies greatly improve in going from QFF to MQFF, SQFF, and MSQFF with substituted potentials showing 26, 32, and 52% improvement, respectively, compared with the unsubstituted force field.

Regarding individual deviations in fundamental transitions we find a similar pattern as in water. Unsubstituted mode frequencies are almost not affected, while symmetric and antisymmetric stretch modes transitions show significant improvements in their frequencies. We again find that the substitution of the symmetric mode by Morse coordinates produces a noticeable improvement in antisymmetric mode transition, and vice versa, which is caused by the substituted potentials producing a better representation of the strongly coupled regions between these two modes for our test cases.

Overtone bands again show a steady improvement relative to QFF in going from MQFF to SQFF and to MSQFF, although somewhat less so than for the fundamental bands (2, 24, and 33%, respectively). Unsubstituted modes frequencies are, again, little affected, and substituted bands show all better accordance with experiment, with the sole exception of the antisymmetric mode overtone frequency in MQFF which worsens significantly, and counterweights the 37 cm^{-1} cut on the deviation of the symmetric mode with respect to experiment.

TABLE 2 VCI frequencies (cm^{-1}) of fundamental, overtone, and combination bands for formaldehyde using QFF, MQFF, SQFF, and MSQFF model PES at the MP2/cc-pVTZ electronic structure level of theory

States		Model potential				Experimental[a]
		QFF	MQFF	SQFF	MSQFF	
ν_1		2833 (51)	2820 (38)	2825 (43)	2811 (29)	2782
ν_2		1739 (7)	1739 (7)	1739 (7)	1739 (7)	1746
ν_3		1515 (15)	1515 (15)	1513 (13)	1514 (14)	1500
ν_4		1170 (3)	1171 (4)	1169 (2)	1170 (3)	1167
ν_5		2882 (39)	2861 (18)	2855 (12)	2845 (2)	2843
ν_6		1250 (0)	1251 (1)	1249 (1)	1250 (0)	1250
1_2		5628 (165)	5591 (128)	5607 (144)	5581 (118)	5463
2_2		3461 (11)	3463 (9)	3462 (10)	3462 (10)	3472
3_2		3028 (30)	3027 (29)	3023 (25)	3025 (27)	2998
4_2		2336 (8)	2333 (5)	2334 (6)	2331 (3)	2328
5_2		5741 (90)	5522 (129)	5700 (49)	5692 (41)	5651
6_2		2498 (2)	2496 (0)	2495 (1)	2494 (2)	2496
$1_1\ 2_1$		4572 (43)	4561 (32)	4564 (35)	4552 (23)	4529
$1_1\ 3_1$		4326 (72)	4316 (62)	4313 (59)	4306 (52)	4254
$1_1\ 4_1$		3978 (38)	3980 (40)	3968 (28)	3968 (28)	3940
$(1_1\ 5_1{:}1_1\ 3_1\ 6_1)_L$		5361 (72)	5464 (31)	5465 (32)	5415 (18)	5433
$(1_1\ 5_1{:}1_1\ 3_1\ 6_1)_H$		5671 (140)	5606 (75)	5616 (85)	5575 (44)	5531
$1_1\ 6_1$		4057	4054	4044	4041	
$2_1\ 3_1$		3246 (7)	3246 (7)	3244 (5)	3245 (6)	3239
$2_1\ 4_1$		2901 (5)	2902 (4)	2900 (6)	2901 (5)	2906
$2_1\ 5_1$		4593 (21)	4484 (88)	4474 (98)	4466 (106)	4572
$2_1\ 6_1$		3011 (10)	3012 (11)	3010 (9)	3008 (7)	3001
$3_1\ 4_1$		2684 (17)	2684 (17)	2680 (13)	2682 (15)	2667
$3_1\ 5_1$		4326	4374	4365	4360	
$3_1\ 6_1$		2724 (5)	2726 (7)	2718 (1)	2714 (5)	2719
$4_1\ 5_1$		3978 (18)	3890 (106)	3873 (123)	3868 (128)	3996
$4_1\ 6_1$		2423 (1)	2423 (1)	2420 (2)	2421 (1)	2422
$5_1\ 6_1$		4057 (26)	4084 (1)	3911 (172)	3905 (178)	4083
MAD	Fundamentals	19	14	13	9	
	Overtones	51	50	39	34	
	Comb. Bands	34	34	48	44	
	Overall	34	33	38	34	

Experimental values are also given for reference. Absolute deviations from experimental values are shown in parentheses. Mean absolute deviation (MAD) values are given at the bottom for fundamental, overtone, and combination bands separately, as well as for the whole set.
[a]References [44, 47].

Interestingly, combination bands show an average trend contrary to the rest of the spectrum, as the MAD increases noticeably for substituted relative to unsubstituted force fields. Analyzing individual deviations we see that combination bands that do not include substituted modes show very little change in any of the substituted force fields, relative to QFF. Moreover, bands including the symmetric mode, show some improvement in their frequencies.

We consider $1_1 5_1$ and $1_1 3_1 6_1$ combination bands separately, as they present us with a good test case to see if the seemingly good quality of the substituted force fields between the symmetric and antisymmetric proton stretch modes, as depicted in Figures 2 and 3, translate into better frequencies. These bands are particularly difficult to model, as they are involved in a strong Fermi resonance. Indeed the assignment of this couple of bands has been the subject of some controversy in the past.[6,47–51] These two states are strongly coupled, resulting in VCI states almost evenly mixed, so the usual method of assignment consisting in naming a state by its dominant contribution is rendered meaningless as their composition is extremely sensitive to small changes in the potential representation. Here, we adopt the naming convention of Yagi et al.[51] and simply call them $(1_1 5_1 : 1_1 3_1 6_1)_L$ and $(1_1 5_1 : 1_1 3_1 6_1)_H$ for the lower and higher energy states disregarding their exact VCI coefficients composition.

As shown in Table 2, the frequencies obtained by using the doubly substituted force field (MSQFF) are in much better agreement with experiment than those obtained with simple normal coordinates, with an error recovery of 75% and 68% for $(1_1 5_1 : 1_1 3_1 6_1)_L$ and $(1_1 5_1 : 1_1 3_1 6_1)_H$, respectively. Singly substituted force fields MQFF and SQFF both produce intermediate results for these states.

These results contrast with those of combination bands $2_1 5_1$, $4_1 5_1$, and $5_1 6_1$ which frequencies are in fairly good agreement with experiment within the QFF representation, but show large errors in substituted force fields. The reason for this can be found by analyzing the corresponding bidimensional slices of the potential in substituted and unsubstituted QFF representations, and comparing them to the *ab initio* potential energy grid in the same coordinate range.

Figure S5 and S6 in the Supporting Information[47] show such bi dimensional energy surfaces and Supporting Information Figures S7 and S8, the corresponding percentage error surfaces, respectively, for additional pairs of modes including symmetric or antisymmetric stretching modes. For all the states in question it can be seen that although in the *ab initio* potential grid the energy rises smoothly in all directions, the QFF approximation produces surfaces where the potential tends rapidly to negative infinity at some or all the corners of the plots (i.e., V(+,+), V(+,-), V(-,+), and V(-,-)) . Comparing the QFF with the SQFF surface it is possible to infer that the use of sinh substitution exacerbates this artifact, effectively shrinking the usable region along the unsubstituted coordinate. This produces surfaces that plunge faster into negative infinity than its unsubstituted version. The fact that the region of potential surface directly along the substituted coordinate actually shows lower error than its unsubstituted counterpart supports this reasoning.

5 | CONCLUSIONS

In the present study, we have presented a novel QFF substitution scheme using a combination of sinh and Morse coordinates for the calculation of anharmonic vibrational energies using variational methods, that is well suited for the use of cartesian normal coordinates as the base coordinate system.

We showed that the use of sinh coordinates is suggested by assuming that the potential is Morse-like along individual bond stretching degrees of freedom. Moreover, the scheme is easily applicable to molecules with more than two equivalent hydrogen atoms, by using a similar procedure as the one outlined in section 2.

We implemented this scheme in a new program recently developed by us called QUMVIA (Quantum mechanical vibrational analysis), which also implements VSCF and VCI variational vibrational structure methodologies for the calculation of anharmonic vibrational energies, and is freely available to the community under GNU GPLv3 license.

Formulas for the analytical integrals using sinh, as well as Morse coordinates, necessary for VSCF/VCI calculations as implemented in QUMVIA are also derived and presented in this work.

The accuracy of the sinh-Morse coordinate substitution scheme is tested by comparing one and two-dimensional sections of the substituted QFFs with unsubstituted QFF and *ab initio* grids using two well-studied benchmark molecules as test cases, water and formaldehyde.

We also calculated VSCF/VCI vibrational transition frequencies for unsubstituted as well as substituted QFFs. We found a very promising error reduction in the frequencies of fundamental and overtone transitions of symmetric and antisymmetric modes, with little change in the frequencies of transitions associated with other modes.

We found, however, that care should be taken in the case of combination bands including only one sinh-substituted mode, as these show an increase in the error. This problem is not observed in any other case, although it does highlight the importance of analyzing the effect of new coordinate substitution schemes over more than one dimension to characterize the limits of its validity.

Overall, sinh-Morse coordinate substitution scheme is found to constitute a promising alternative to QFFs based fully on simple cartesian normal coordinates, given the fact that QFF substitution schemes in general do not require any extra computational effort above that necessary for building the normal QFF.

Also, the use of sinh-Morse scheme is especially advantageous when the underlying code uses analytical integrals, as other proposed coordinate substitution schemes for normal coordinates[10] require numerical methods for their calculation, and is specifically adapted for its use with normal coordinates as the base coordinate system for the QFF. A more throughout testing of the proposed scheme is underway to establish its accuracy using a greater variety of molecular symmetries and sizes.

ACKNOWLEDGMENTS

D.J.A.A. would like to express his gratitude to Professor R. M. S. Alvarez for her support, as well as Prof. Dario Estrin and Prof. Adrian Roitberg for many enlightening discussions, and also acknowledge CONICET for a doctoral fellowship.

REFERENCES

[1] K. Yagi, T. Taketsugu, K. Hirao, M. S. Gordon, *J. Chem. Phys.* **2000**, *113*, 1005.
[2] S. Carter, S. J. Culik, J. M. Bowman, *J. Chem. Phys.* **1997**, *107*, 10458.
[3] J. O. Jung, R. B. Gerber, *J. Chem. Phys.* **1996**, *105*, 10332.
[4] G. Li, S.-W. Wang, C. Rosenthal, H. Rabitz, *J. Math. Chem.* **2001**, *30*, 1.
[5] D. Strobusch, C. Scheurer, *J. Chem. Phys.* **2014**, *140*, 74111.
[6] D. C. Burleigh, A. B. McCoy, E. L. Sibert, *J. Chem. Phys.* **1996**, *104*, 480.
[7] K. C. Thompson, M. A. Collins, *J. Chem. Soc. Faraday Trans.* **1997**, *93*, 871.
[8] X.-G. Hu, T.-S. Ho, H. Rabitz, *Chem. Phys. Lett.* **1998**, *288*, 719.
[9] R. Ramakrishnan, G. Rauhut, *J. Chem. Phys.* **2015**, *142*, 154118.
[10] R. Burcl, S. Carter, N. C. Handy, *Chem. Phys. Lett.* **2003**, *373*, 357.
[11] O. Christiansen, *Phys. Chem. Chem. Phys.* **2007**, *9*, 2942.
[12] M. Keçeli, T. Shiozaki, K. Yagi, S. Hirata, *Mol. Phys.* **2009**, *107*, 1283.
[13] R. C. Fortenberry, X. Huang, A. Yachmenev, W. Thiel, T. J. Lee, *Chem. Phys. Lett.* **2013**, *574*, 1.
[14] J. Ischtwan, M. A. Collins, *J. Chem. Phys.* **1994**, *100*, 8080.
[15] M. J. T. Jordan, K. C. Thompson, M. A. Collins, *J. Chem. Phys.* **1995**, *102*, 5647.
[16] K. C. Thompson, M. J. T. Jordan, M. A. Collins, *J. Chem. Phys.* **1998**, *108*, 8302.
[17] K. Yagi, T. Taketsugu, K. Hirao, *J. Chem. Phys.* **2002**, *116*, 3963.
[18] S. Y. Lin, P. Zhang, J. Z. H. Zhang, *Chem. Phys. Lett.* **2013**, *556*, 393.
[19] T. J. Frankcombe, M. A. Collins, D. H. Zhang, *J. Chem. Phys.* **2012**, *137*, 144701.
[20] C. Crespos, M. A. Collins, E. Pijper, G. J. Kroes, *Chem. Phys. Lett.* **2003**, *376*, 566.
[21] O. Christiansen, *Phys. Chem. Chem. Phys.* **2012**, *14*, 6672.
[22] R. Dawes, D. L. Thompson, A. F. Wagner, M. Minkoff, *J. Chem. Phys.* **2008**, *128*, 84107.
[23] C. E. Dateo, T. J. Lee, D. W. Schwenke, *J. Chem. Phys.* **1994**, *101*, 5853.
[24] R. C. Fortenberry, X. Huang, T. D. Crawford, T. J. Lee, *J. Phys. Chem. A* **2013**, *117*, 9324.
[25] R. C. Fortenberry, X. Huang, J. S. Francisco, T. D. Crawford, T. J. Lee, *J. Chem. Phys.* **2011**, *135*, 134301.
[26] R. C. Fortenberry, X. Huang, T. D. Crawford, T. J. Lee, *J. Phys. Chem. A* **2014**, *118*, 7034.
[27] J. K. G. Watson, *Mol. Phys.* **1968**, *15*, 479.
[28] W. Meyer, P. Botschwina, P. Burton, *J. Chem. Phys.* **1986**, *84*, 891.
[29] S. Carter, N. C. Handy, *J. Chem. Phys.* **1987**, *87*, 4294.
[30] S. Carter, N. C. Handy, *Chem. Phys. Lett.* **2002**, *352*, 1.
[31] J. M. Bowman, *J. Chem. Phys.* **1978**, *68*, 608.
[32] J. M. Bowman, K. Christoffel, F. Tobin, *J. Phys. Chem.* **1979**, *83*, 905.
[33] J. M. Bowman, M. Bowman, *Acc. Chem. Res.* **1986**, *19*, 202.
[34] J. M. Bowman, T. Carrington, H.-D. Meyer, *Mol. Phys.* **2008**, *106*, 2145.
[35] T. C. Thompson, D. G. Truhlar, *Chem. Phys. Lett.* **1980**, *75*, 87.
[36] K. M. Christoffel, J. M. Bowman, *Chem. Phys. Lett.* **1982**, *85*, 220.
[37] S. Carter, J. M. Bowman, N. C. Handy, *Theor. Chem. Acc.* **1998**, *100*, 191.
[38] D. M. Chemes, D. J. Alonso de Armiño, E. H. Cutin, H. Oberhammer, N. L. Robles, *J. Mol. Struct.* **2017**, *1127*, 191.
[39] A. L. Páez Jerez, D. J. Alonso de Armiño, N. L. Robles, *New J. Chem.* **2015**, *39*, 9894.
[40] I. P. Hamilton, J. C. Light, *J. Chem. Phys.* **1986**, *84*, 306.
[41] M. Neff, G. Rauhut, *J. Chem. Phys.* **2009**, *131*, 124129.
[42] D. J. Alonso de Armiño, QUMVIA GitHub homepage. https://github.com/diegoarmino/qumvia (accessed April 16, **2017**).
[43] Gaussian 03, Revision C.02, M. J. Frisch, G. W. Trucks, H. B. Schlegel, G. E. Scuseria, M. A. Robb, J. R. Cheeseman, J. A. Montgomery, Jr, T. Vreven, K. N. Kudin, J. C. Burant, J. M. Millam, S. S. Iyengar, J. Tomasi, V. Barone, B. Mennucci, M. Cossi, G. Scalmani, N. Rega, G. A. Petersson, H. Nakatsuji, M. Hada, M. Ehara, K. Toyota, R. Fukuda, J. Hasegawa, M. Ishida, T. Nakajima, Y. Honda, O. Kitao, H. Nakai, M. Klene, X. Li, J. E. Knox, H. P. Hratchian, J. B. Cross, V. Bakken, C. Adamo, J. Jaramillo, R. Gomperts, R. E. Stratmann, O. Yazyev, A. J. Austin, R. Cammi, C. Pomelli,

J. W. Ochterski, P. Y. Ayala, K. Morokuma, G. A. Voth, P. Salvador, J. J. Dannenberg, V. G. Zakrzewski, S. Dapprich, A. D. Daniels, M. C. Strain, O. Farkas, D. K. Malick, A. D. Rabuck, K. Raghavachari, J. B. Foresman, J. V. Ortiz, Q. Cui, A. G. Baboul, S. Clifford, J. Cioslowski, B. B. Stefanov, G. Liu, A. Liashenko, P. Piskorz, I. Komaromi, R. L. Martin, D. J. Fox, T. Keith, M. A. Al-Laham, C. Y. Peng, A. Nanayakkara, M. Challacombe, P. M. W. Gill, B. Johnson, W. Chen, M. W. Wong, C. Gonzalez, J. A. Pople, Gaussian, Inc., Wallingford CT, **2004**.

[44] T. Shimanouchi, *Tables of Molecular Vibrational Frequencies Consolidated*, National Bureau of Standards **1972**, *1*, 1–60.

[45] D. F. Smith, J. Overend, *Spectrochim. Acta Part A Mol. Spectrosc.* **1972**, *28*, 471.

[46] R. A. McClatchey, W. S. Benedict, S. A. Clough, D. E. Burch, R. F. Calfee, *AFCRL Atmospheric Absorption Line Parameters Compilation*. (No. AFCRL-TR-73-0096). Air Force Cambridge Research Labs HANSCOM AFB MA. **1973**, 1–90.

[47] R. J. Bouwens, J. A. Hammerschmidt, M. M. Grzeskowiak, A. Tineke, P. M. Yorba, W. F. Polik, **1996**, *104*, 460.

[48] J. M. L. Martin, T. J. Lee, P. R. Taylor, *J. Mol. Spectrosc.* **1993**, *160*, 105.

[49] M. Aoyagi, S. K. Gray, M. J. Davis, *J. Opt. Soc. Am. B* **1990**, *7*, 1859.

[50] S. Carter, N. Pinnavaia, N. C. Handy, *Chem. Phys. Lett.* **1995**, *240*, 400.

[51] K. Yagi, C. Oyanagi, T. Taketsugu, K. Hirao, *J. Chem. Phys.* **2003**, *118*, 1653.

SUPPORTING INFORMATION

Additional Supporting Information may be found online in the supporting information tab for this article.

How to cite this article: Alonso de Armiño DJ, Bustamante CM. A quartic force field coordinate substitution scheme using hyperbolic sine coordinates. *Int J Quantum Chem.* 2017;117:e25390. https://doi.org/10.1002/qua.25390